MJFAS
Malaysian Journal of Fundamental and Applied Sciences

Nasir *et al.* | Malaysian Journal of Fundamental and Applied Sciences, Vol. 21 (2025) 2790–2796

RESEARCH ARTICLE

The Electrical Characteristics of a Filamentary Discharge of Capillary Guided Corona Discharge Plasma Jet

Norhayati Mohd Nasir[a], Seong Ling Yap[b,*], Lian Kuang Lim[b], Seong Shan Yap[c]

[a]Faculty of Bioeconomic and Health Sciences Universiti Geomatika Malaysia, 54200 Kuala Lumpur, Malaysia; [b]Department of Physics, University of Malaya, 50603 Kuala Lumpur, Wilayah Persekutuan Kuala Lumpur, Malaysia; [c]Department of Physics, Xiamen University, Jalan Sunsuria, Bandar Sunsuria, 43900 Sepang, Selangor Malaysia

Abstract Nonthermal plasma jet device has been employed as a sterilisation means and effectively eradicate various microorganisms. Plasma jet device for this purpose has been most successful with a He or argon gas flow and often characterized by a long plasma plume. The expensive working gases such as helium and the gas control system however limits many practical applications. Capillary guided plasma jet (CGPJ) studied here employed at ambient air generated a constant funnel-shaped plasma plume of about 6 mm. The plasma jet plume has been optimised with different inner diameter capillary quartz tube and gap distance. The dissipative power was around 1.5 to 4.5 W. The effectiveness of the CGPJ in utilizing ambient air enables continuous sterilization and microbial inactivation processes, making it a promising approach for the treatment of medical devices and intricate implants. However, its direct application to living cells may pose safety concerns and may require further investigation and adjustment to enhance biocompatibility and safety for in vivo applications.

Keywords: Nonthermal Plasma, Plasma jet, Filamentary Discharge, Gas flow.

Introduction

Plasma as a means of sterilisation has been effectively eradicate various microorganisms due to its composition of an ionized gas which formed through the liberation of electrons from gas molecules. It has been tremendously explored ever since its empirical stage [1] and routinely used at low temperature for material processing [2]. Atmospheric pressure plasma is non-thermal with partial ionization that the plasma jet consists of ambient gas, electrons, ions, reactive species and emissions from the excited molecules. The plasma constituent which predominantly consists of various reactive species react with bacterial cell wall via oxidative stress mechanism or through internal cellular destruction. Reactive oxygen species (ROS) produced in air discharge caused strong oxidative stress that could damage bacterial cell wall by inducing lipid peroxidation, enzyme inactivation or causing DNA cleavage [3][4]. Radicals help in the reduction of microcirculatory disorders and accelerate fibroblast proliferation and collagen synthesis with the correct plasma dosage [5]. However discharge in air often turns filamentary [6]and specific consideration is needed to produce a homogenous air plasma [3]. Most often used gases are helium and argon, that sometime mixed with some percentage of air.

The coaxial plasma jet design hardly generates plumes, and as the breakdown of non uniform distribution, point or wire electrode occur, streamers of charges possibly propagated to the opposite electrode producing ionisation wave channel [7]. Most of the time, discharges are formed in the flow of inert gases such as helium [8], [9] or argon gas [10], [11]. It is often characterized by a long plasma plume. Ambient air is generally electronegative consisting of nitrogen, oxygen, and water vapour, which induce electron attachments and efficiently quench nitrogen metastable species. Approach to generate non-thermal plasma jet with ambient air also need to prevent high current arc and keep the plasma jet at low temperature. Otherwise, air non-thermal plasma jet is most attractive with the copious species generated with a long life time such as various N_2 metastables, reactive nitrogen and oxygen species.

***For correspondence:**
yapsl@um.edu.my

Received: 16 April 2025
Accepted: 13 August 2025

In this study, a non-thermal plasma jet is generated in ambient air which have been topic of interest [12]. The effect of gap distance between and the influence on the filamentary discharge have been investigated.

In this study, a capillary guided plasma jet (CGPJ) plume is generated using ambient air as the plasma forming gas. In a plasma jet assisted by feed gas, the breakdown voltage and the plume length are dependent on the electrode-quartz tube configuration [13] and gas flow rate[14]. In the current configuration, the gas flow rate is zero, and the central electrode has no charge, so the plume length was determined on the capillary tube. The placement of the outer ring electrode closed the discharge circuit of the electrode-quartz tube configuration in a non-transferred mode operation. The momentum of electron and ion currents in the confined space produced the extended plasma plume without feed gas. This configuration of CGPJ has been employed in transfer mode operation and effective in the eradication of chronic wound bacteria[15], [16]. The equivalent dose for the CGPJ in inducing cells proliferation has also been determined through multiple linear regression method [5]. The CGPJ in ambient air has all the essential species in the plasma effluent for bacterial inactivation in medical device sterilisation and suitable for continuous application.

Materials and Methods

CGPJ Setup

The The CGPJ was constructed in a coaxial geometry as shown in Figure 1 and powered by a high-voltage plasma driver of 25 kV_{pp} maximum. The AC frequency, with a maximum frequency of 27 kHz, was tuned to match the load. The CGPJ is made up of a central electrode, a 200 μm diameter enamelled copper wire connected to the high-voltage plasma driver, and it is enclosed by a quartz capillary tube. The quartz capillary tube has a high insulating strength of 7×10^7 ohm.cm and a dielectric constant of 3.76. The inner pin electrode was centered in the capillary tube, with its tip sharpened, and placed at a small distance before the orifice of the capillary tube. A copper ring of 5 mm width was used as the ground electrode and placed outside the capillary tube at a position near the orifice. The gap distance, d was varied between 3 and 5 mm while the length between the tip of sharpest electrode to the end of tube was constant at 3 mm. This quartz capillary acts as the dielectric barrier that limit the discharge current and sustain charges along its inner and outer surface. Three different quartz capillary tube with the inner diameter of 1, 2 and 3 mm have been used in this study. The voltage across the electrodes was measured with a Tektronix P6015A high-voltage probe at 1000 times attenuation. The discharge current was measured via a sensing resistor of 1 Kohm connected to the ground electrode. Voltage and current signals were recorded simultaneously by a digital oscilloscope.

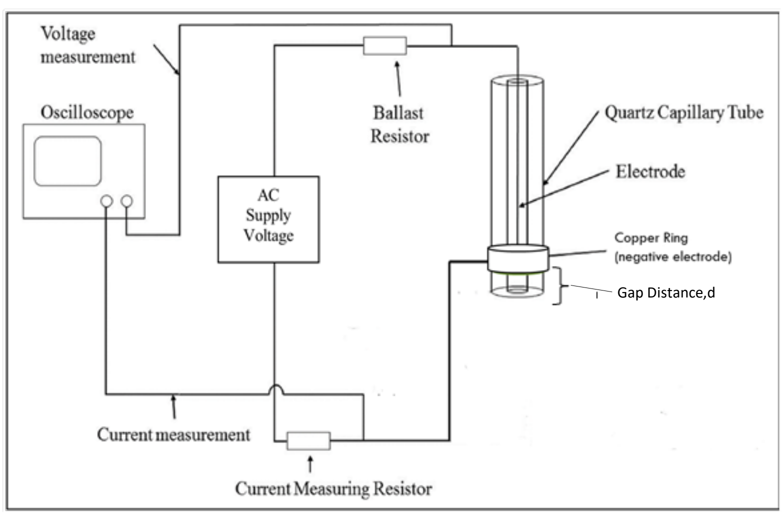

Figure 1. Schematic of CGPJ device

The electrical power consumed in the CGPJ discharge was evaluated using the Manley method [12]. A monitoring capacitor was used in replacement of the sensing resistor for charge measurement. The charge-voltage (Q-V) diagram or Lissajous figure was plotted from the time profile of the voltage V(t) against the charge measured. The power dissipated was determined by the Lissajous figure. The instantaneous power varied with the voltage waveform following Equation (1):

$$P\,(t) = V(t).i(t) = V(t).C_m \frac{dV_m}{dt} \tag{1}$$

The average power dissipated in a full discharge cycle is given by the integration of the Q-V diagram, as in Equation (2):

$$\bar{P} = \frac{1}{T}\int_0^T V(t).C_m \frac{dV_m(t)}{dt}dt = \frac{1}{T}\int_0^T V(t).C_m dV_m\,(t) = \frac{1}{T}\oint V(t)dQ(t) \tag{2}$$

Results and Discussion

CGPJ Electrical Characteristics

The discharge obtained with the 1 mm inner diameter capillary tube required a threshold voltage of 15 kV_{pp}, compared to 18 kV_{pp} and 22 kV_{pp} when 2 mm and 3 mm capillary tubes were employed. The pin electrode created a local enhancement of the electric field at the central electrode while the Quartz capillary tube insulate around the central pin and provided surface charges to sustain the plasma plume. The CGPJ device discussed further in this study employed a quartz tube of 1 mm inner diameter. The 1 mm inner diameter quartz capillary tube leaves a region of 400 um around the central electrode sufficient limit diffusion of the plasma plume [6]. In a plasma jet assisted by feed gas, the breakdown voltage and the plume length are dependence on the electrode-quartz tube configuration and the flow rate. In the current configuration gas flow rate is zero, central electrode remains uncharged that the plume length was determined on the capillary tube. The placement of the outer ring electrode closed the discharge circuit of the electrode-quartz tube configuration in a non-transferred mode operation. The momentum of electron and ion currents in the confined space produced the extended plasma plume without feed gas. Applied voltage was increased from 5 kV_{pp} to 25 kV_{pp} at 27 kHz, by which breakdown was obtained. The variation in the gap distance from 3 mm to 5 mm resulted in a change in the longest plasma plume lengths from 1 mm to 6 mm with the respective optimum discharge parameters.

At the 5 kV_{pp} applied voltage, electron avalanches occurred, with some current spikes measured while the discharge remained dim. The discharge with emission in the violet region in the capillary tube was observed at 10 kV_{pp}. Further increase in the applied voltage has resulted in electron avalanche in the forward direction, with observable plasma plume. The visible plasma plume extended to several millimetres in the ambient without feed gas. The plasma plume observed resemble a diffuse and continuous glow superimposed with some dynamic current filaments. This discharge characteristic was not the same as that observed in a flow assisted plasma jet that comprises of many filaments. The filaments bifurcated into thinner branches in the ambient and the discharge current registered the random current spikes in each half cycle when voltage rose above 1 kV At 5 kV_{pp} applied voltage, electron avalanche occurred with some current spikes measured while the discharge remained dim (Figure 2a). The discharge with emission in the violet region in the capillary tube was observed at 10 kV_{pp}. (Figure 2b)

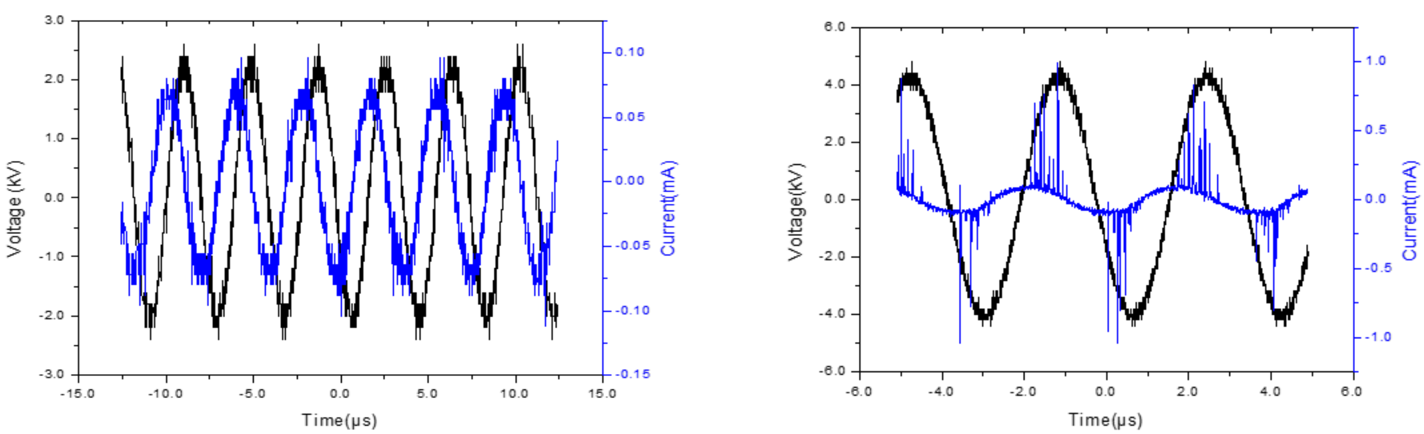

(a) (b)

Figure 2(a). At 5 kV_{pp} applied voltage, electron avalanche occurred with some current spikes measured while the discharge remained dim, 2(b): More current spikes occurred as the voltage increases to 10kV_{pp}

The discharge filaments in the CGPJ occurred in the ambient would have all the species from air as the plasma reactor. During the positive cycle, the negative charges accumulated on the central electrode, while the ionization wave pushed on the capillary wall. In the reversal cycle the electrons pushed to the capillary wall were deposited on the dielectric surface. These memory charges accumulated on the dielectric surface compensated the applied electric field giving a lower measured voltage of about 15kV_{pp}. During the fall of the voltage cycle, excited species near the surface of inner electrode decayed with light emission giving bright zone near the electrode tip. The formation of current pulses are similar to that reported [10]. The number of current pulses measured in the discharge current positive and negative cycles are about the same. In the negative cycle, slightly more current pulses has been observed when voltage was increased to 25 kV_{pp}. The number of current pulses and their respective amplitudes in the positive and negative current cycles are summarized in Figure 3.

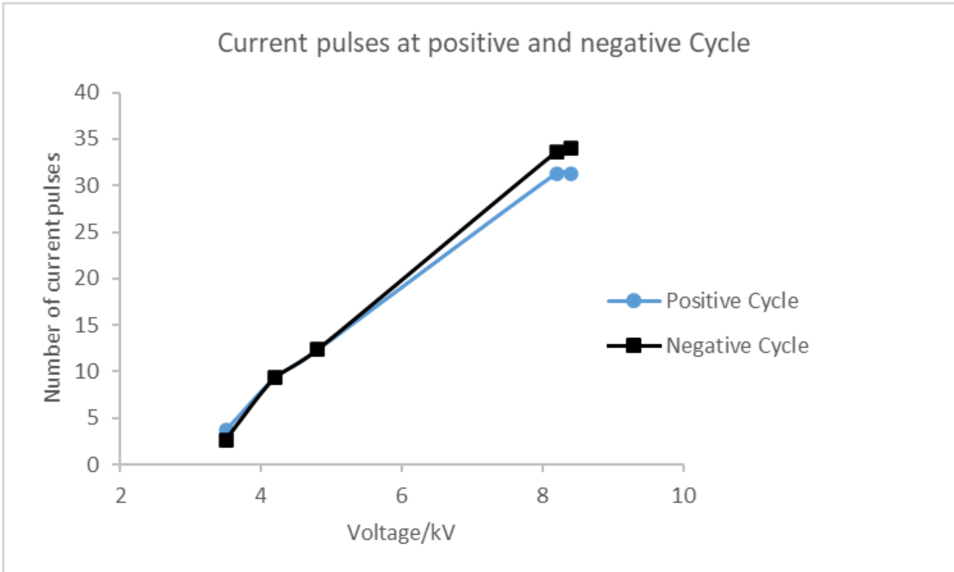

Figure 3. Number of current pulses averaged for the positive and negative cycles

This discharge characteristic was not the same as that observed in a flow assisted plasma jet that comprises of many filaments. The filaments bifurcated into thinner branches in the ambient and the discharge current registered the random current spikes in each half cycle when voltage rose above 1 kV. Similar discharge behaviour has been reported that the characteristics was analysed by using a gated ICCD and optical emission measurements [11]. The ICCD results suggested that only a single filament was produced in each current pulse and the maximum electron density in the filament was estimated to 11.2 $x10^{15}cm^{3}$.

The CGPJ created a plasma reactor in ambient air supporting rich reactions whereby the collision of energetic electrons with particles in the air resulted in many different excitation levels of atoms and molecules. The plasma plume appeared bright violet, extended to a length of approximately 6 mm from the orifice, diffused outward like a funnel-shaped torch, and dimmed at further distances, Figure 4 (a), (b) and (c)

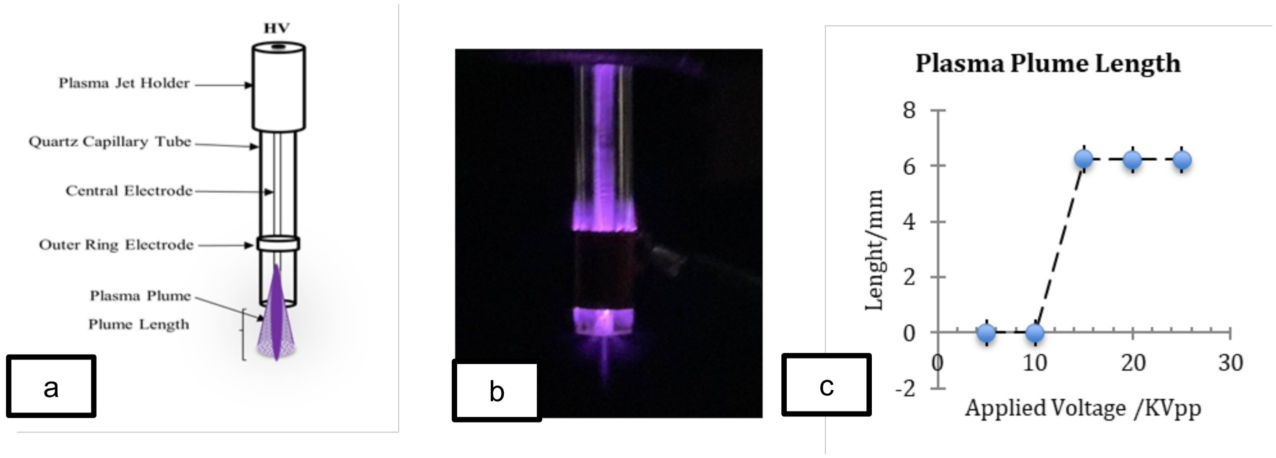

Figure 4. The CGPJ device (b) photograph showing the discharge plume (c) CGPJ plume length

The QV Lissajous figure corresponding to the applied voltages of 10kV$_{pp}$ to 25kV$_{pp}$ are plotted in Figure 5.

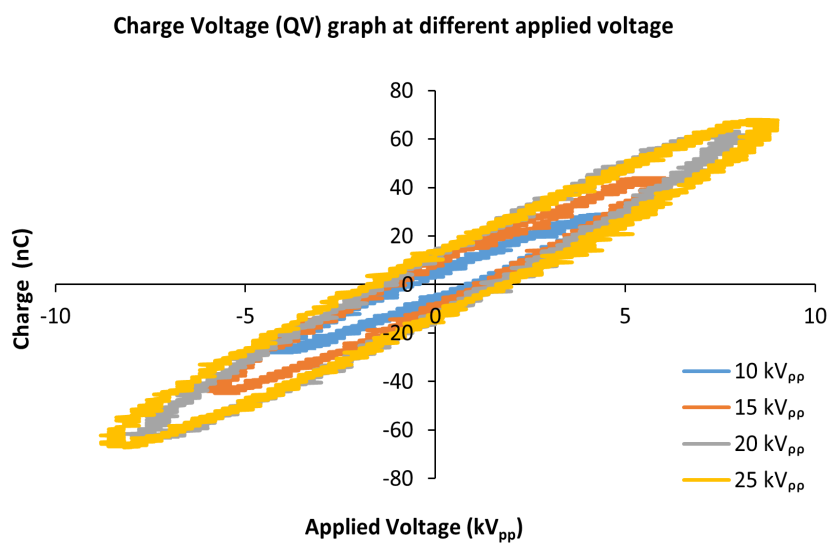

Figure 5. The Lissajous curve for the applied voltages 10kV$_{pp}$ to 25kV$_{pp}$ CGPJ device (b) photograph showing the discharge plume (c) CGPJ plume length.

A typical parallelogram representing a filamentary mode DBD discharge as described by the Manley's theory [9] was not the case here. The Lissajous figures resembled an ellipse diagram similar to that observed in surface dielectric barrier discharge. The gradual increase capacitance following the curve was due to the gradual expansion of the plasma plume along the capillary tube similar to the configuration of a plasma actuator. In addition to that the plasma plume expanded outward from the orifices of the CGPJ in the short phase between the current pulses. The gradient of the Lissajous curve was the effective capacitance εdiel increasing with the expansion of the plasma plume. The memory charges on the dielectric surface reached to the maximum at voltage peaks. The effective capacitance estimated at 8.42 pF for 20 kVpp. The power dissipated in the plasma plume was determined for the applied voltage of 10 kV$_{pp}$ to 25 kV$_{pp}$ are presented in Figure 5. The extrapolated line indicates a linear increment of discharge from 10 kV$_{pp}$ to 15 kV$_{pp}$. The power correspond to the plasma plume was about 1.8 Watt at 15 kV$_{pp}$ and made a jump to 4.0 Watt at 20 kV$_{pp}$. The additional power of about 1.4 Watt correspond to the more intense plasma plume at 20 kV$_{pp}$. The power consumed in the CGPJ remained low, below 5 W for 25 kV$_{pp}$ Figure 6.

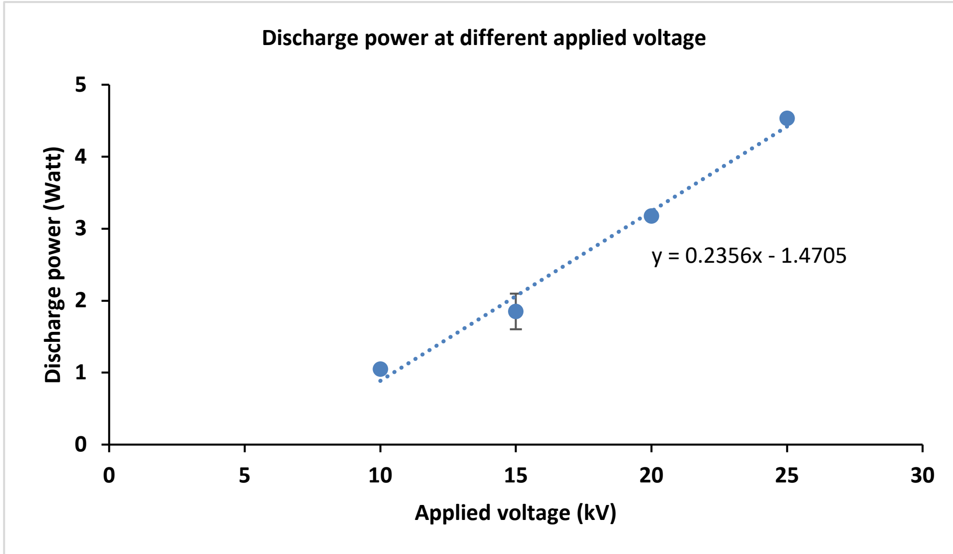

Figure 6. Power dissipated determined from the Lissajous figure diagram

A linear relationship between discharge power and applied voltage was observed in the region where no sample present. A higher applied voltage leads to increased discharge of power, thereby enabling more energy to be transferred, which allows the plume to propagate over a longer distance. The use of the CGCD on grounded samples shall enhances the plasma jet, resulting in increased discharge power and a more intense plasma (Nishime *et al*., 2020).

Conclusions

Ambient plasma jet was produced by a CGPJ driven by high voltage high frequency AC discharge. The plasma driver operated at discharge frequency of 27 kHz was found best matching the plasma load. The plasma plume properties are principally determined by the applied voltage. The plasma plume has a length of 6 mm with applied voltage of 10 kV_{pp} and turn brighter with applied voltage of 15 kV_{pp} or above with practically same length. The number of current pulses increased with the applied voltage. Current pulses formed in the positive and negative cycles are symmetric following the oscillation of the electrons and ion waves in the capillary tube. The power dissipated was around 1.5 to 4.5 W when operated at 5kV_{pp} to 25kV_{pp}. The CGPJ operated as an oscillator of the high energy electrons, with memory charges deposited on the capillary tube in the reversal cycle of the high voltage. Expansion of the discharge zone was driven by high charge density, producing a funnel shape plasma plume outside the orifice of the capillary tube.

Conflicts of Interest

The author(s) declare(s) that there is no conflict of interest regarding the publication of this paper.

Acknowledgment

This work is part of a research project, TRGS/1/2020/UM/02/2/3) supported by the Ministry of Higher Education, Malaysia.

References

[1] Von Woedtke, T., Reuter, S., Masur, K., & Weltmann, K. D. (2013). *Plasmas for medicine*. Elsevier B.V. https://doi.org/10.1016/j.physrep.2013.05.005

[2] Laroussi, M. (2005). Low temperature plasma-based sterilization: Overview and state-of-the-art. Plasma

Processes and Polymers. https://doi.org/10.1002/ppap.200400078.
[3] Bogaerts, A., *et al*. (2015). Multi-level molecular modelling for plasma medicine. *Journal of Physics D: Applied Physics, 49*(5). https://doi.org/10.1088/0022-3727/49/5/054002.
[4] Graves, D. B. (2012). The emerging role of reactive oxygen and nitrogen species in redox biology and some implications for plasma applications to medicine and biology. *Journal of Physics D: Applied Physics, 45*(26), 263001. https://doi.org/10.1088/0022-3727/45/26/263001.
[5] Yap, S. L., Norhayati, M. N., Teow, S. Y., & Yap, S. S. (2022, February). Equivalent dose of atmospheric plasma jet on inducing cell proliferation in human fibroblast cell. *Proceedings of the IEEE International Conference on Plasma Science (ICOPS)*, 199–199. https://doi.org/10.1109/icops37625.2020.9717576.
[6] Tay, W. H., Yap, S. L., & Wong, C. S. (2014). Electrical characteristics and modeling of a filamentary dielectric barrier discharge in atmospheric air (Ciri Elektrik dan Model Suatu Nyahcas Dielektrik Berpenghadang dalam Udara Atmosfera). *Journal of Science and Technology*.
[7] Lu, X., Naidis, G. V., Laroussi, M., & Ostrikov, K. (2014). Guided ionization waves: Theory and experiments. *Physics Reports*. Elsevier. https://doi.org/10.1016/j.physrep.2014.02.006.
[8] Pang, B., *et al.* (2021). Discharge mode transition in a He/Ar atmospheric pressure plasma jet and its inactivation effect against tumor cells in vitro. *Journal of Applied Physics, 130*(15). https://doi.org/10.1063/5.0063135.
[9] Shaker, M. M., Mohammad, R. K., & Fuliful, F. K. (2023). Investigation on characteristics of atmospheric pressure helium plasma jet by using different Pyrex tubes thickness. *Journal of Physics Conference Series*.
[10] Acharya, T. R., Jang, M., Lee, G. J., & Choi, E. H. (2023). A comprehensive study on the synthesis, characteristics, and catalytic applications of submerged hydrogen-mixed argon plasma-synthesized silver nanoparticles. *Current Applied Physics, 56*, 36–46. https://doi.org/10.1016/j.cap.2023.09.003.
[11] Baldanov, B. B., Ranzhurov, T. V., Semenov, A. P., & Gomboeva, S. V. (2019). Cold atmospheric argon plasma jet source and its application for bacterial inactivation. *Journal of Theoretical and Applied Physics, 13*(2), 95–99. https://doi.org/10.1007/s40094-019-0326-3.
[12] Lu, X., Laroussi, M., & Puech, V. (2012). On atmospheric-pressure non-equilibrium plasma jets and plasma bullets. *Plasma Sources Science and Technology, 21*(3), 034005. https://doi.org/10.1088/0963-0252/21/3/034005
[13] R. T. P., & Kar, S. (2023). Effect of an additional floating electrode on radio frequency cross-field atmospheric pressure plasma jet. *Scientific Reports, 13*(1). https://doi.org/10.1038/s41598-023-37805-7.
[14] Nishime, T. M. C., Wagner, R., & Kostov, K. G. (2020). Study of modified area of polymer samples exposed to a He atmospheric pressure plasma jet using different treatment conditions. *Polymers, 12*(5), 1028. https://doi.org/10.3390/polym12051028.
[15 Mohd Nasir, N., Lee, B. K., Yap, S. S., Thong, K. L., & Yap, S. L. (2016). Cold plasma inactivation of chronic wound bacteria. *Archives of Biochemistry and Biophysics, 605*, 76–85. https://doi.org/10.1016/j.abb.2016.03.033.
[16] Muttiah, B., Mohd Nasir, N., Mariappan, V., Vadivelu, J., Vellasamy, K. M., & Yap, S. L. (2024). Targeting colon cancer and normal cells with cold plasma-activated water: Exploring cytotoxic effects and cellular responses. *Physics of Plasmas, 31*(8). https://doi.org/10.1063/5.0216291.